Improving the Model Convective Storm Quantitative Precipitation Nowcasting by Assimilating State Variables Retrieved from Multiple-Doppler Radar Observations

YU-CHIENG LIOU, JIAN-LUEN CHIOU, WEI-HAO CHEN, AND HSIN-YU YU

Department of Atmospheric Sciences, National Central University, Jhongli City, Taiwan

(Manuscript received 7 October 2013, in final form 14 May 2014)

ABSTRACT

This research combines an advanced multiple-Doppler radar synthesis technique with the thermodynamic retrieval method, originally proposed by Gal-Chen, and a moisture/temperature adjustment scheme, and formulates a sequential procedure. The focus is on applying this procedure to improve the model quantitative precipitation nowcasting (QPN) skill in the convective scale up to 3 hours. A series of (observing system simulation experiment) OSSE-type tests and a real case study are conducted to investigate the performance of this algorithm under different conditions.

It is shown that by using the retrieved three-dimensional wind, thermodynamic, and microphysical parameters to reinitialize a fine-resolution numerical model, its QPN skill can be significantly improved. Since the Gal-Chen method requires the horizontal average properties of the weather system at each altitude, utilization of in situ radiosonde(s) to obtain this additional information for the retrieval is tested. When sounding data are not available, it is demonstrated that using the model results to replace the role played by observing devices is also a feasible choice. The moisture field is obtained through a simple, but effective, adjusting scheme and is found to be beneficial to the rainfall forecast within the first hour after the reinitialization of the model.

Since this algorithm retrieves the unobserved state variables instantaneously from the wind measurements and directly uses them to reinitialize the model, fewer radar data and a shorter model spinup time are needed to correct the rainfall forecasts, in comparison with other data assimilation techniques such as four-dimensional variational data assimilation (4DVAR) or ensemble Kalman filter (EnKF) methods.

OBJECTIVE

Better nowcasting

Convective storms

Assimilation method

Multiple-Doppler radar

KEYWORDS

OSSE

observing system simulation experiment

Assimilation method:

3DVAR*, 4DVAR, EnKF, ⋯

*VAR = variational data assimilation

**ENKF = ensemble Kalman filter

METHODOLOGY

1. Multiple-Doppler wind synthesis method
2. modified thermodynamic retrieval algorithm
3. moisture/temperature adjustment scheme

Multiple-Doppler wind synthesis method

變分法 vs 傳統風場反演

- ✓ 允許Baseline OK
- ✓ 一次處理多座雷達 OK
- ✓ 允許渦度收支分析 OK
- ✓ 較彈性的風場上下邊界
- ✓ 模式探空補足雷達死角
- ✓ 風場資訊可直接給熱力反演

modified thermodynamic retrieval algorithm

源自Gal-Chen (1978)，
再加上尤和廖(2009) 的水相變化

基本場 (0)：降水未發生前的狀態
擾動量 (′)： 降水系統發生時，大氣狀態與基本場的差異量。

標準化氣壓 $\pi = C_p \left(\frac{p}{p_{00}}\right)^{R/C_p}$ (2.13)

modified thermodynamic retrieval algorithm

多雷達三維風場 ▸ π′ - < π′ > ▸ 探空 ▸ π′

$$\frac{1}{\theta_{v0}}\left[\frac{\partial u}{\partial t}+\vec{V}\cdot\nabla u-fv+turb(u)\right]=-\frac{\partial \pi'}{\partial x}\equiv -F \qquad (2.8)$$

$$\frac{1}{\theta_{v0}}\left[\frac{\partial v}{\partial t}+\vec{V}\cdot\nabla v+fu+turb(v)\right]=-\frac{\partial \pi'}{\partial y}\equiv -G \qquad (2.9)$$

反演
氣壓擾動

$$\frac{1}{\theta_{v0}}\left[\frac{\partial w}{\partial t}+\vec{V}\cdot\nabla w+turb(w)+gq_r\right]=-\frac{\partial \pi'}{\partial z}+g\frac{\theta_c'}{\theta_0\theta_{v0}}\equiv -H \qquad (2.10)$$

$$\theta_{v0}=\theta_0(1+0.61q_{v0}) \qquad (2.11)$$

$$\frac{35}{2}\log M+43.1=Z(dBZ) \qquad (2.12)$$

$$M=\rho\times q_r$$

$$\theta_c'=\theta'+(0.61q_v'-q_c)\theta_0 \qquad (2.15)$$

$$J=\iint\left[\left(\frac{\partial \pi'}{\partial x}-F\right)+\left(\frac{\partial \pi'}{\partial y}-G\right)\right]dxdy \qquad (2.16)$$

$$\frac{\partial^2 \pi'}{\partial x^2}+\frac{\partial^2 \pi'}{\partial y^2}=\frac{\partial F}{\partial x}+\frac{\partial G}{\partial y} \qquad (3.25)$$

$$\pi'=0 \qquad (3.26)$$

$$\frac{\partial \pi'}{\partial x}=F \quad \frac{\partial \pi'}{\partial y}=G \qquad (3.27)$$

modified thermodynamic retrieval algorithm

反演獲得 $\pi' \blacktriangleright (2.20) \blacktriangleright \theta_c' \blacktriangleright (2.15) \blacktriangleright \theta'$

$$-\frac{\partial \pi'}{\partial z} + g\frac{\theta_c'}{\theta_0 \theta_{v0}} \equiv -H \qquad (2.20)$$

$$\theta_c' = \theta' + (0.61 q_v' - q_c)\theta_0 \qquad (2.15)$$

$$\theta_{v0} = \theta_0(1 + 0.61 q_{v0}) \qquad (2.11)$$

$$\frac{1}{\theta_{v0}}\left[\frac{\partial u}{\partial t} + \vec{V}\cdot\nabla u - fv + turb(u)\right] = -\frac{\partial \pi'}{\partial x} \equiv -F \qquad (2.8)$$

$$\frac{1}{\theta_{v0}}\left[\frac{\partial v}{\partial t} + \vec{V}\cdot\nabla v + fu + turb(v)\right] = -\frac{\partial \pi'}{\partial y} \equiv -G \qquad (2.9)$$

$$\frac{1}{\theta_{v0}}\left[\frac{\partial w}{\partial t} + \vec{V}\cdot\nabla w + turb(w) + g q_r\right] = -\frac{\partial \pi'}{\partial z} + g\frac{\theta_c'}{\theta_0 \theta_{v0}} \equiv -H \qquad (2.10)$$

反演
溫度擾動

moisture/temperature adjustment scheme

利用反演的風場、溫度、氣壓場，檢查網格是否飽和？

圖片：邱(2013)

$q_v' \blacktriangleright \theta' \blacktriangleright (T,Td)_{sfc} \blacktriangleright LCL \blacktriangleright q_{vs} \blacktriangleright q_v' \blacktriangleright \cdots$

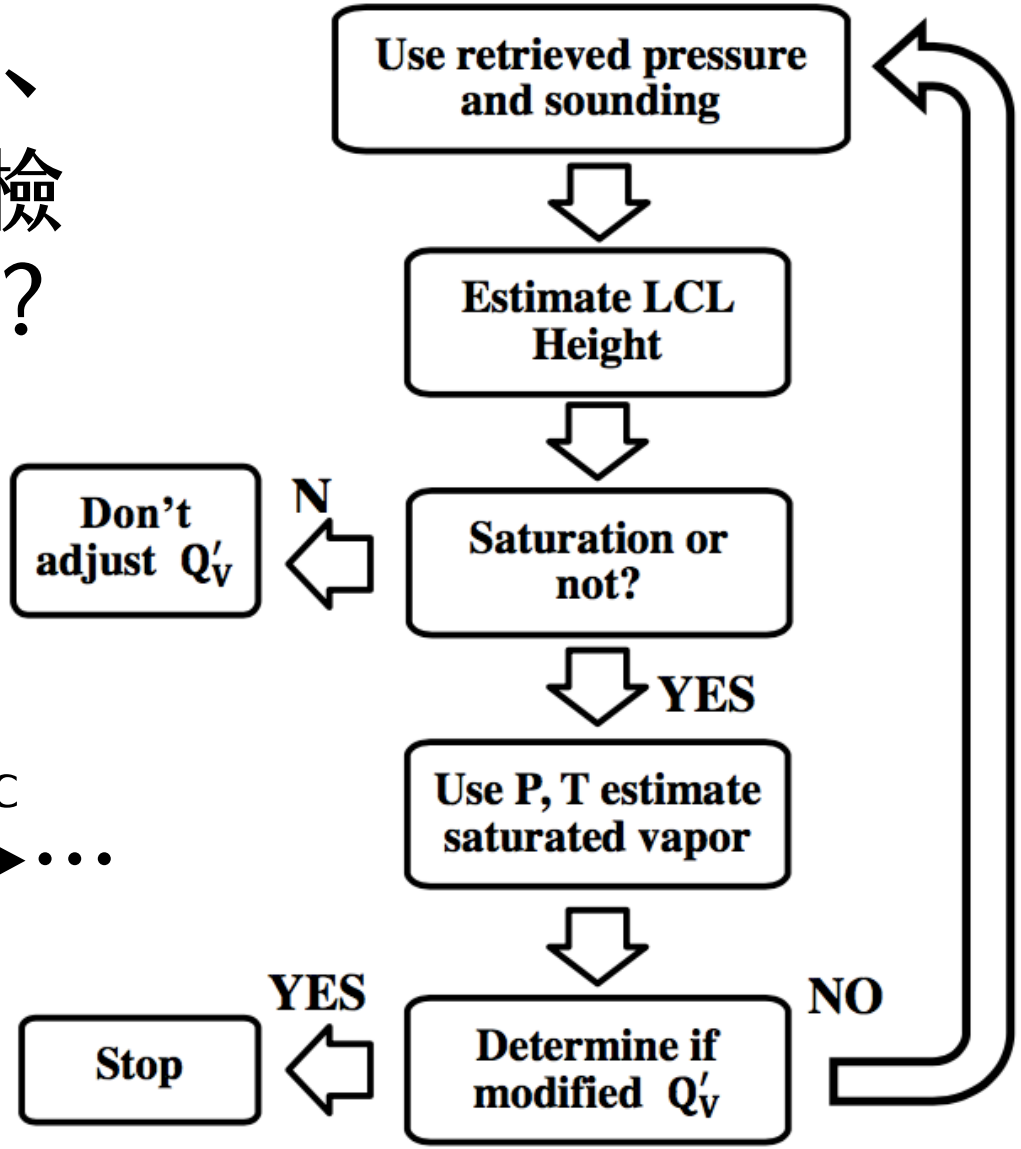

EXPERIMENTS

TABLE 1. Summary of experiments. The experiments using simulated or real data are labeled by "S" and "R," respectively, in the third column.

Expt	Description	Type
TRUE	Simulation of a splitting storm; used as the true atmosphere	S
BKGD	Simulation of a weaker and drier storm, representing an unsuccessful model forecast; also used to provide background information for unretrievable parameters	S
CNTL	A control run with complete wind fields and sounding data available to estimate $\langle p' \rangle$; used as a verification of the retrieval/reinitialization procedure	S
NoSND	Similar to CNTL, but assuming no sounding data, and $\langle p' \rangle$ is provided by BKGD run	S
NoSND2	As in NoSND, but the retrieval/reinitialization procedure without sounding data is applied twice	S
NoQV	As in CNTL, but the moisture field is not adjusted	S
Err_wind	As in CNTL, but perturbations are implemented to imitate errors in wind fields	S
WRF_only	A pure model simulation of the SoWMEX IOP 8 heavy rainfall event; the model is initialized at 0600 UTC, followed by a 9-h simulation until 1500 UTC	R
WRF+rdr_MK	Simulation from WRF_only is updated at 1200 UTC by retrieved state variables using data from three radars; Ma-Kong sounding is also available for estimating $\langle p' \rangle$	R
WRF+rdr_PT	As in WRF+rdr_MK, but the Ping-Tong sounding is used for estimating $\langle p' \rangle$	R
WRF+rdr_MP	As in WRF+rdr_MK, but $\langle p' \rangle$ is estimated by averaging two $\langle p' \rangle$ profiles obtained from Ma-Kong and Ping-Tong soundings	R
WRF+rdr_NoSND	As in WRF+rdr_MK, but $\langle p' \rangle$ is provided using the pressure field from WRF_only	R

EXPERIMENTS

BKGD

0.5K bubble

Half moisture

TRUE

3K bubble

41 x 41 grids

2km(horizontal)

40 vertical layers

Moderate instability

Quarter circle shear profile

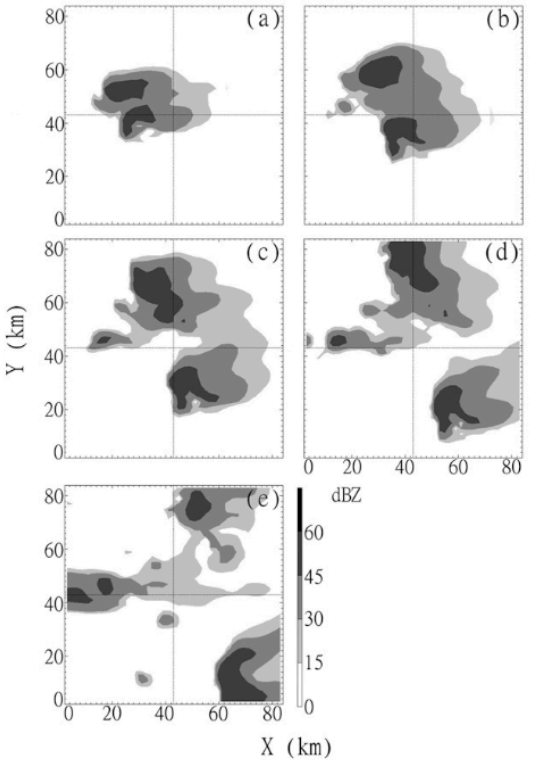

FIG. 1. Simulated radar reflectivity (dBZ, 15-dBZ interval) at Z = 5.0 km from experiment TRUE at (a) 60, (b) 80, (c) 100, (d) 120, and (e)140 min.

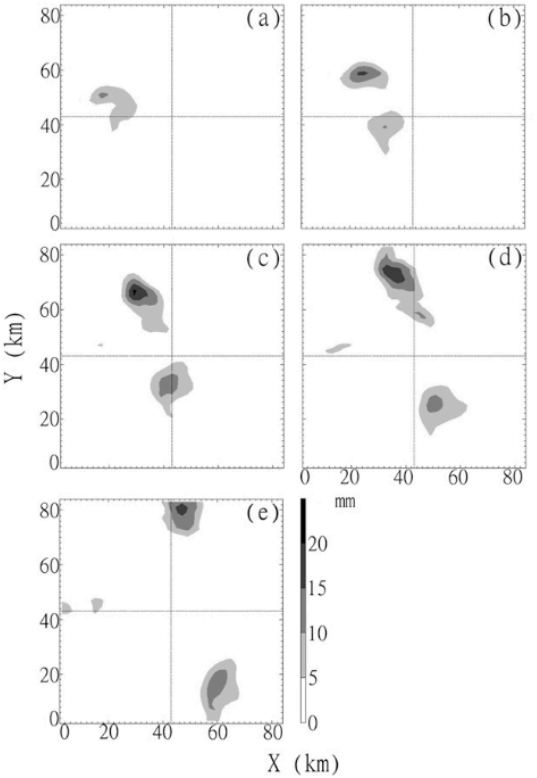

FIG. 2. As in Fig. 1, but for the 5-min accumulated rainfall (5-mm interval) from experiment TRUE.

EXPERIMENTS

TRUE/ CNTL

TRUE

3K bubble
41 x 41 grids
2km(horizontal)
40 vertical layers
Moderate instability
Quarter circle shear profile

CNTL

根據TRUE產生的風場與探空所進行的實驗

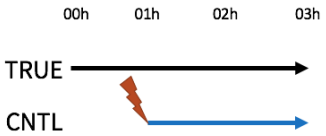

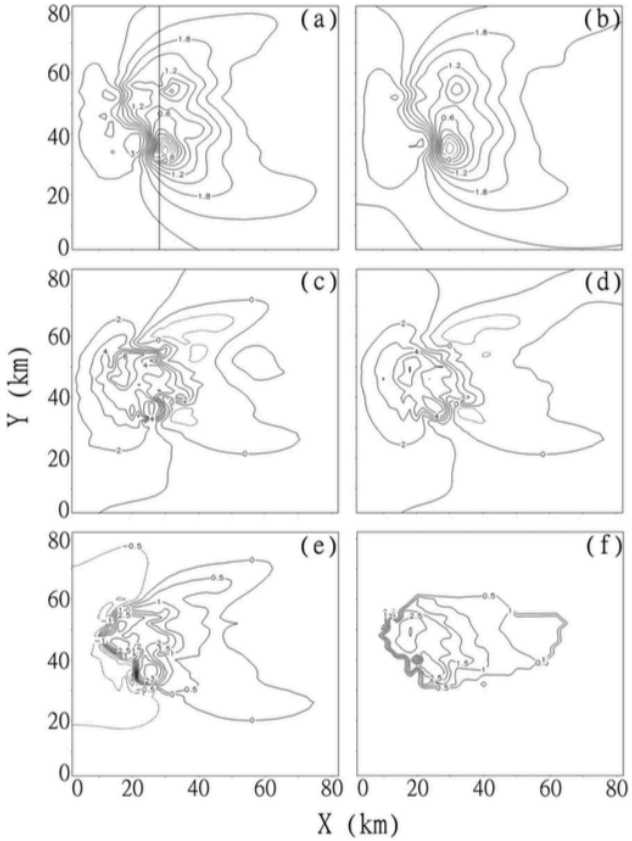

FIG. 3. (left) True and (right) retrieved field over a horizontal plane at $Z = 4.75$ km and $t = 60$ min: (a),(b) pressure perturbation (hPa, 0.3-hPa interval); (c),(d) potential temperature perturbation (K, 1.0-K interval); and (e),(f) water vapor perturbation ($g\,kg^{-1}$, $0.5\,g\,kg^{-1}$ interval). The north–south-oriented line in (a) is the location of the vertical cross section shown in Fig. 4.

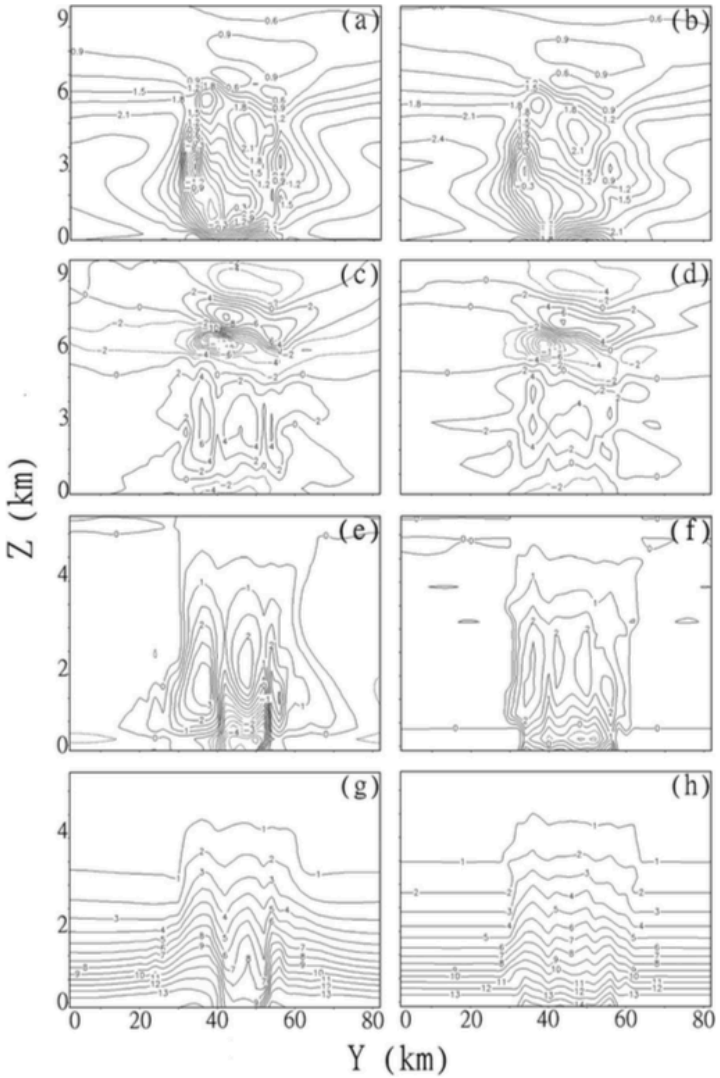

FIG. 4. (left) True and (right) retrieved fields over a north–south vertical cross section at $x = 28$ km and $t = 60$ min: (a),(b) pressure perturbations (hPa, 0.3-hPa interval); (c),(d) potential temperature perturbations (K, 2.0-K interval); (e),(f) water vapor perturbations ($g\,kg^{-1}$, $0.5\,g\,kg^{-1}$ interval); and (g),(h) total water vapor ($g\,kg^{-1}$, $1.0\,g\,kg^{-1}$ interval). Note that in (e)–(h) the vertical domain extends only to $Z = 5.0$ km since there is almost no moisture above this altitude.

EXPERIMENTS

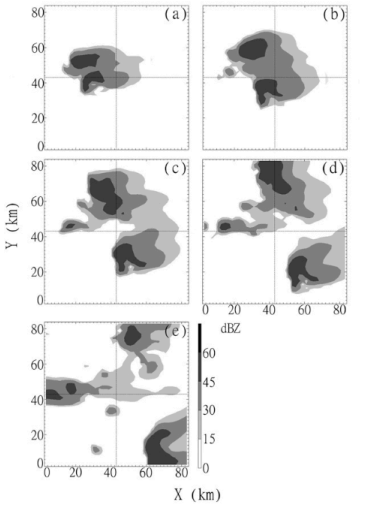

FIG. 1. Simulated radar reflectivity (dBZ, 15-dBZ interval) at Z = 5.0 km from experiment TRUE at (a) 60, (b) 80, (c) 100, (d) 120, and (e) 140 min.

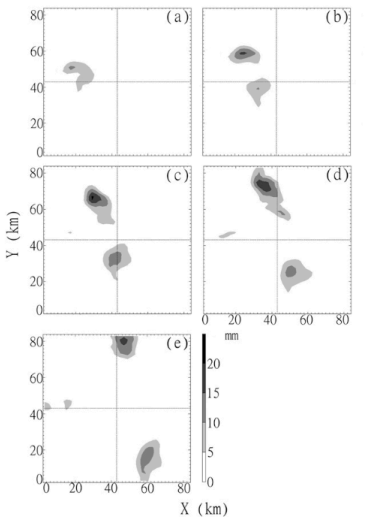

FIG. 2. As in Fig. 1, but for the 5-min accumulated rainfall (5-mm interval) from experiment TRUE.

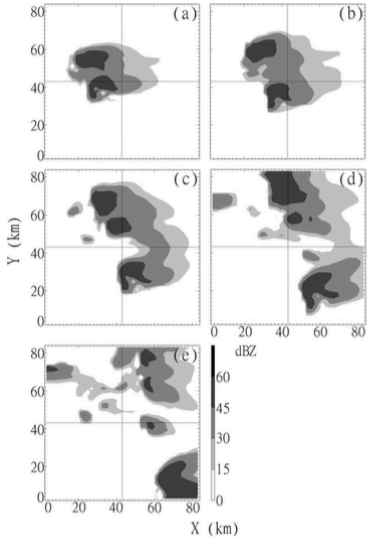

FIG. 5. As in Fig. 1, but from expt CNTL.

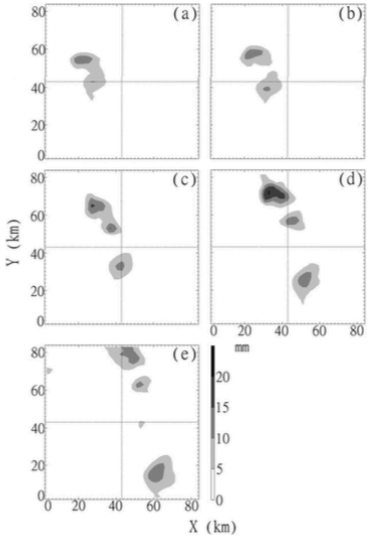

FIG. 6. As in Fig. 2, but from expt CNTL.

CNTL

根據TRUE產生的風場與探空，所進行的實驗

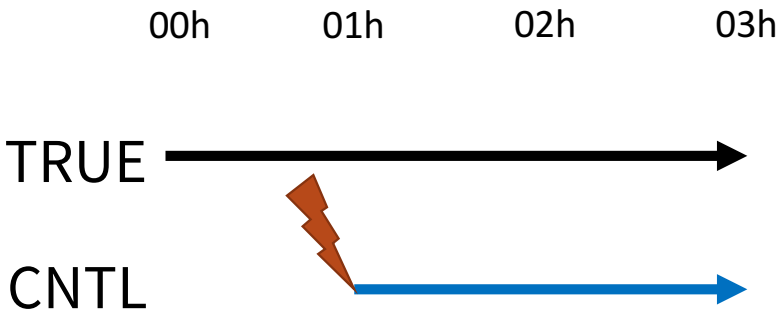

EXPERIMENTS

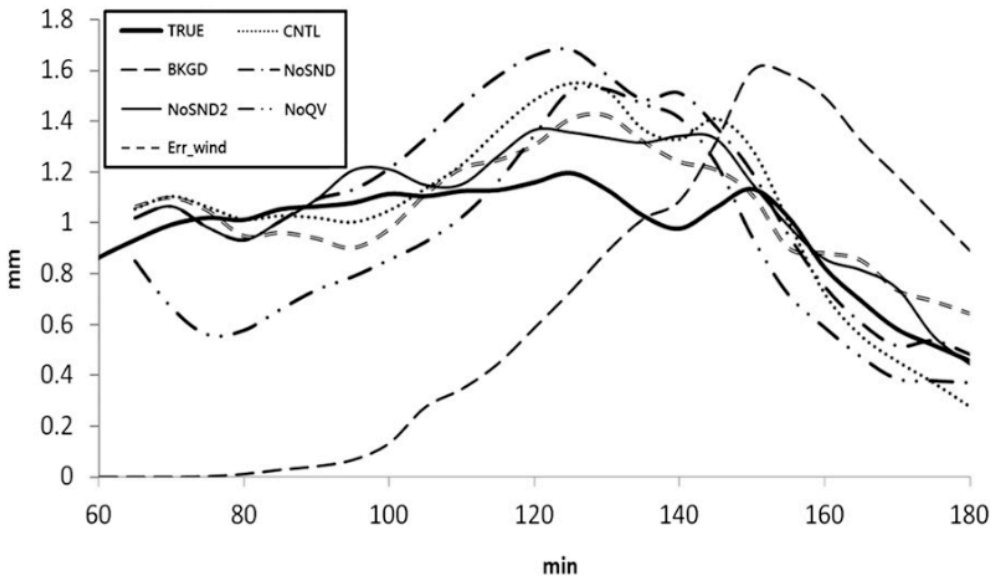

FIG. 7. Time evolution of averaged (over grid points) 5-min accumulated rainfall for all OSSEs.

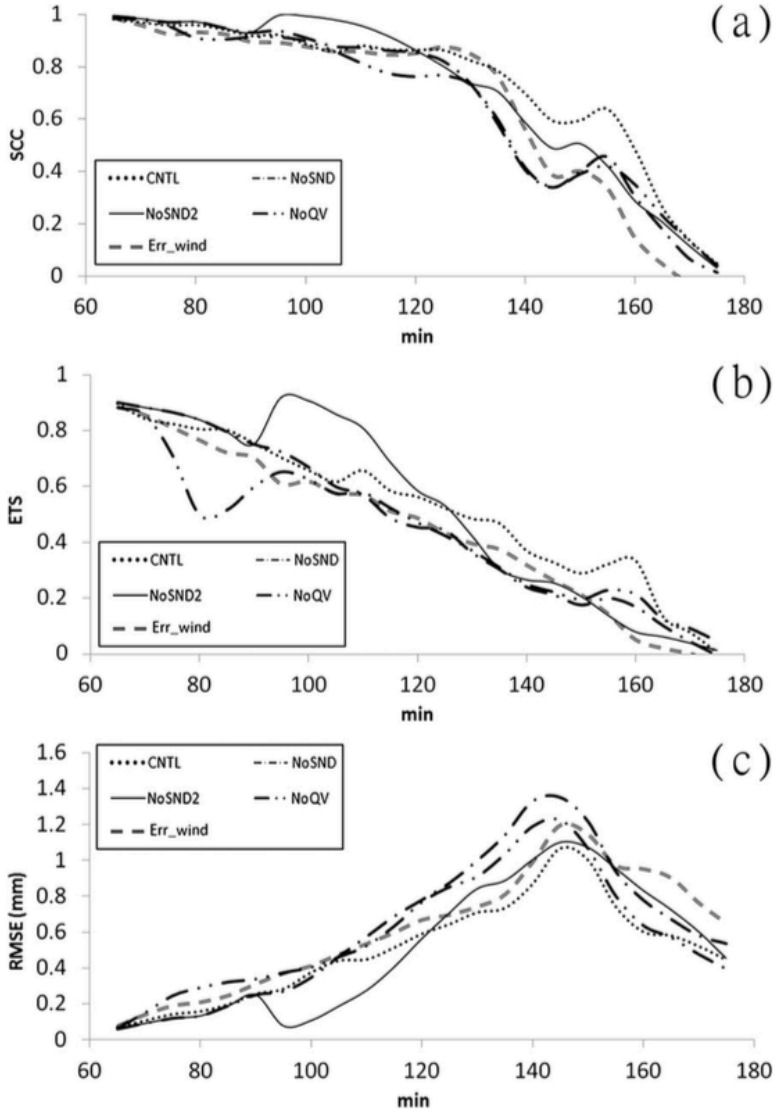

FIG. 8. Time evolution of (a) spatial correlation coefficient (SCC), (b) ETS score with 1.25 mm (5 min)$^{-1}$ threshold, and (c) RMSE between the true (from the TRUE run) and model-forecast 5-min accumulated precipitation for all OSSE data assimilation experiments.

EXPERIMENTS

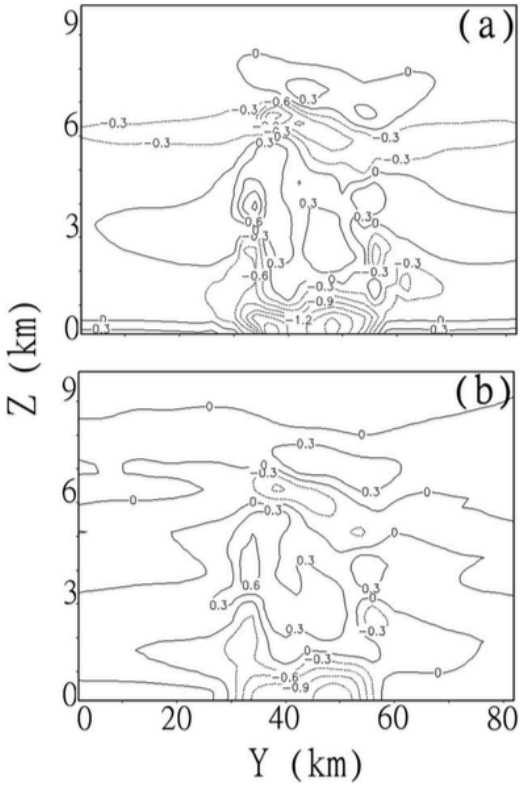

FIG. 9. The vertical gradients of the pressure perturbations (hPa km^{-1}, 0.3 hPa km^{-1} interval) from experiments (a) TRUE and (b) NoSND.

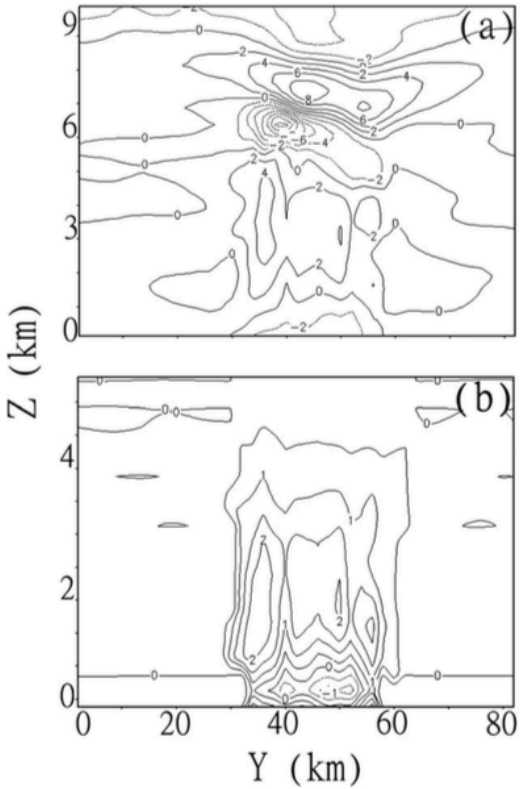

FIG. 10. The retrieved (a) potential temperature (K, 2.0-K interval) and (b) water vapor perturbations (g kg^{-1}, 0.5 k kg^{-1} interval) from experiment NoSND.

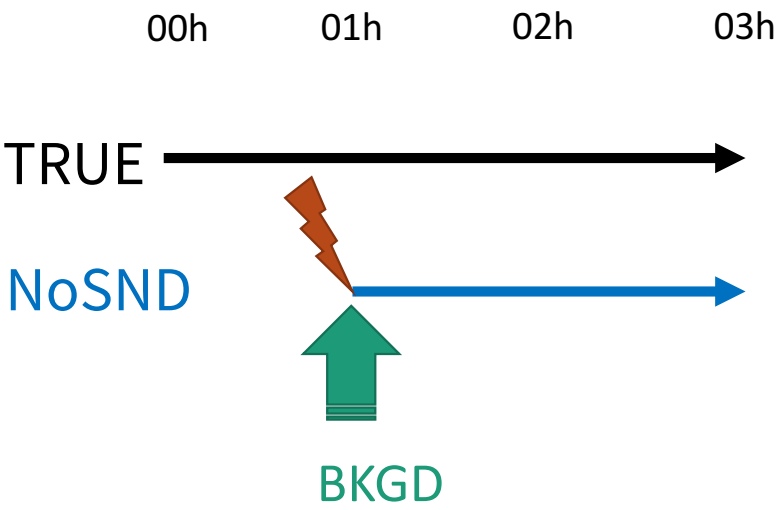

NoSND / NoSND2

沒有探空資料，自行從模式的預報產生。

EXPERIMENTS

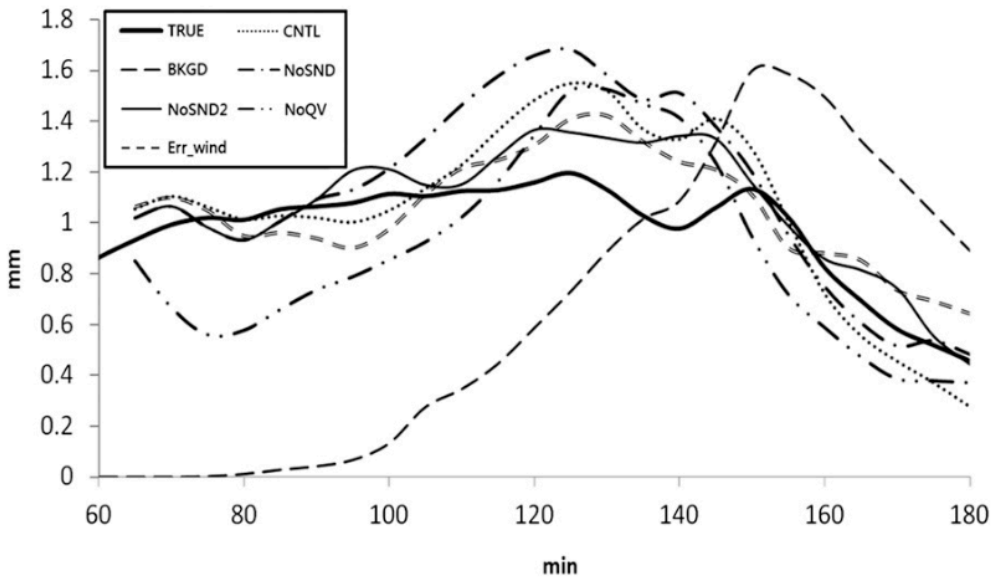

FIG. 7. Time evolution of averaged (over grid points) 5-min accumulated rainfall for all OSSEs.

NoQV / ERR_wind
無水氣調整與
隨機風場誤差

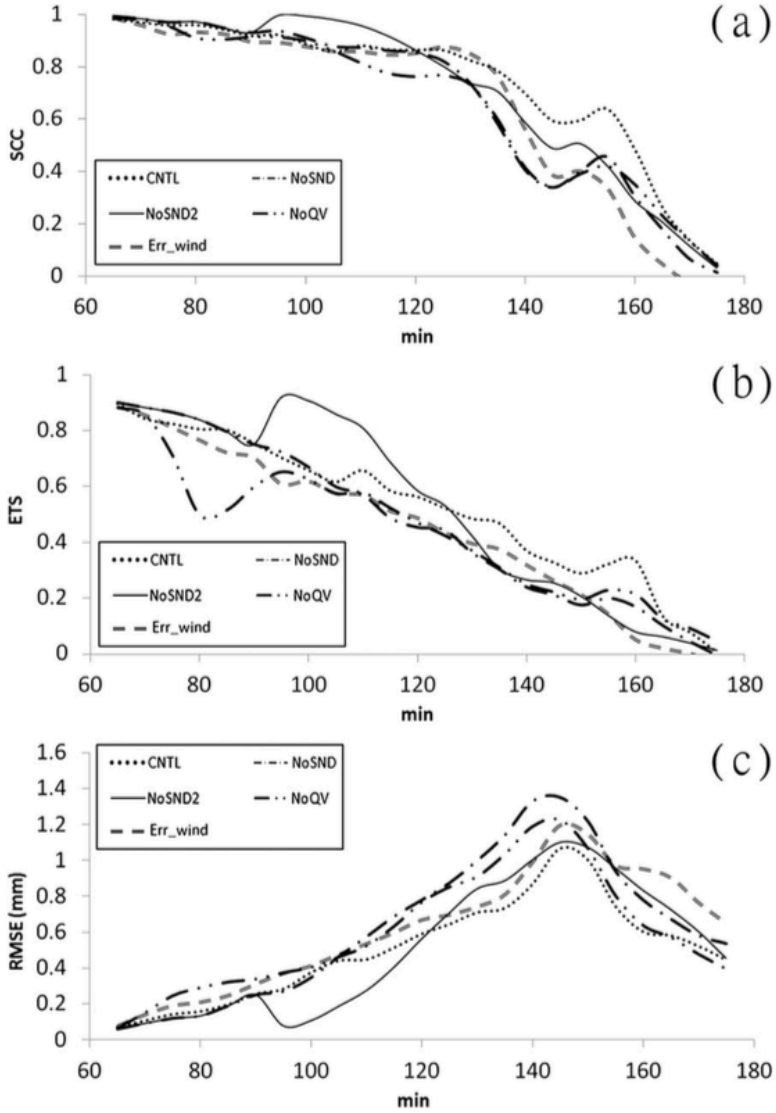

FIG. 8. Time evolution of (a) spatial correlation coefficient (SCC), (b) ETS score with 1.25 mm (5 min)$^{-1}$ threshold, and (c) RMSE between the true (from the TRUE run) and model-forecast 5-min accumulated precipitation for all OSSE data assimilation experiments.

EXPERIMENTS

WRF_only
WRF+rdr_MK
WRF+rdr_PT
WRF+rdr_MP
WRF+rdr_NoSND

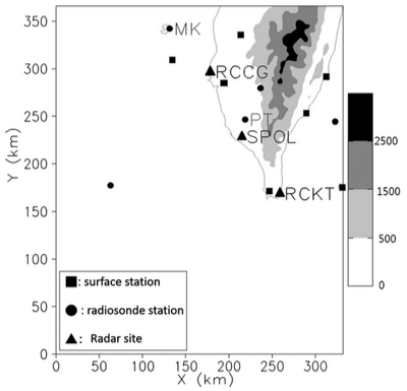

FIG. 11. The locations of data collected from different sources for IOP 8 of 2008 SoWMEX. Triangles indicate three radars (S-POL, RCCG, and RCKT), circles represent radiosondes, and squares stand for surface mesonet stations. The radiosondes released at Ping-Tong (PT) and Ma-Kong (MK) stations are used for the thermodynamic retrieval calculation. The topography is displayed by the gray shading with intervals of 500 and 1000 m.

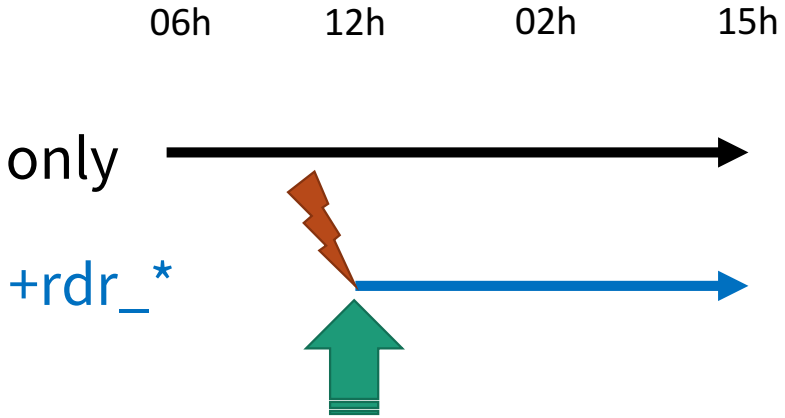

<p'> from MK / MP / both / model

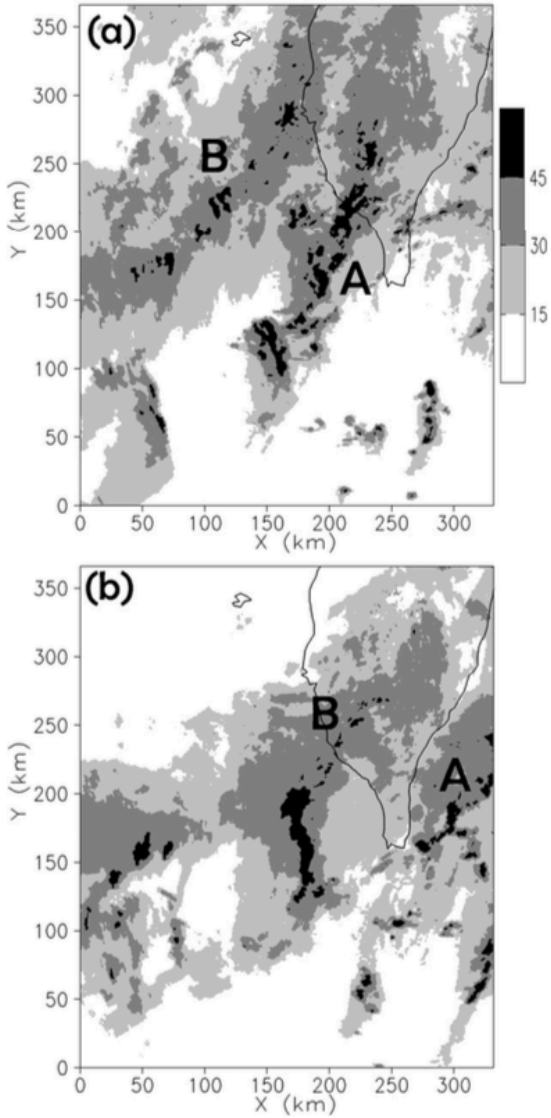

FIG. 12. The observed composite radar reflectivity (max in a column) fields in dBZ (15-dBZ interval) at (a) t = 1200 and (b) t = 1500 UTC.

EXPERIMENTS

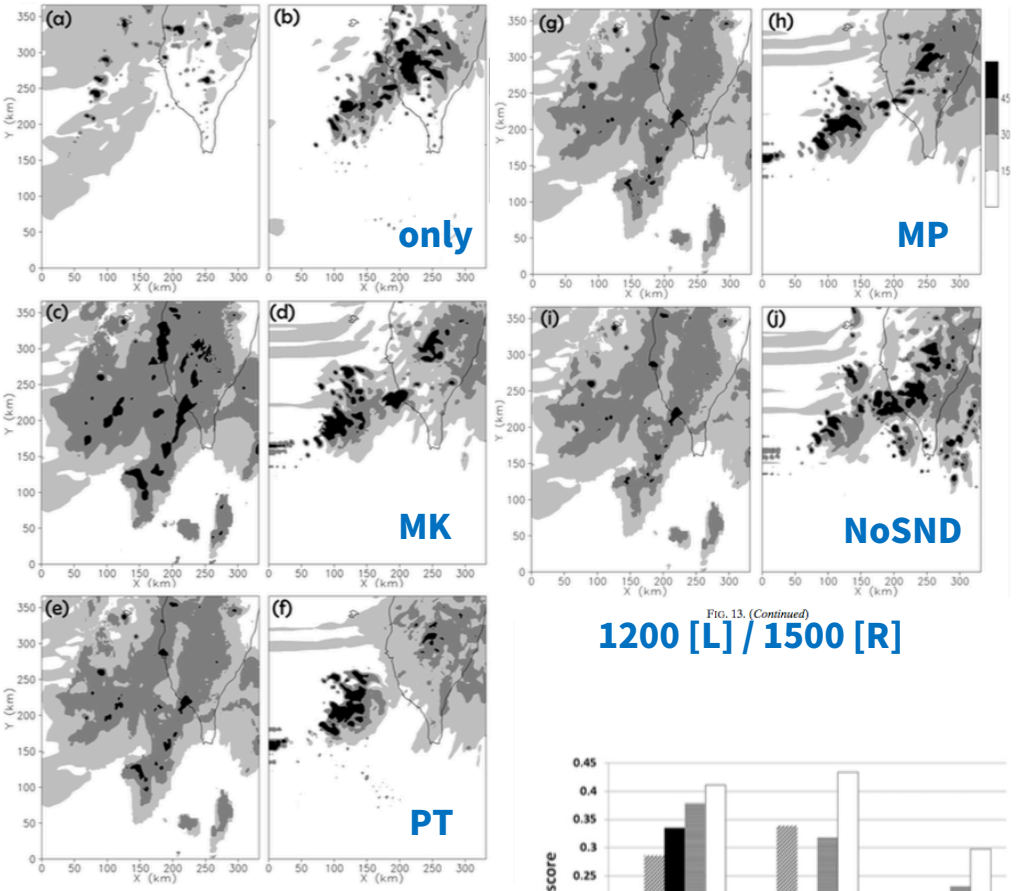

FIG. 13. The model-forecast composite radar reflectivity (max in a column) (dBZ, 15-dBZ interval) from experiments (a),(b) WRF_only; (c),(d) WRF+rdr_MK; (e),(f) WRF+rdr_PT; (g),(h) WRF+rdr_MP; and (i),(j) WRF_NoSND. Results are at (left) t = 1200 and (right) 1500 UTC.

1200 [L] / 1500 [R]

FIG. 13. (*Continued*)

1200 [L] / 1500 [R]

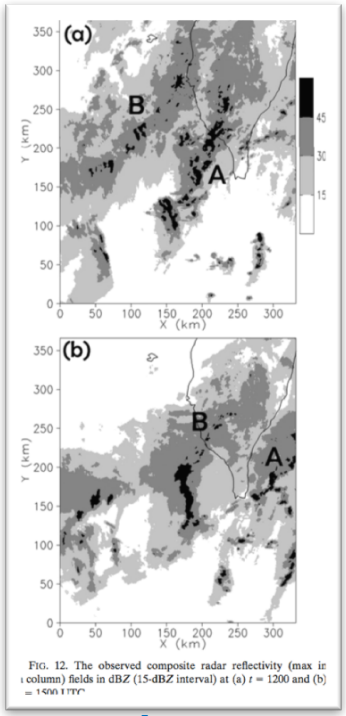

FIG. 12. The observed composite radar reflectivity (max in a column) fields in dBZ (15-dBZ interval) at (a) t = 1200 and (b) = 1500 UTC

obs 1200
obs 1500

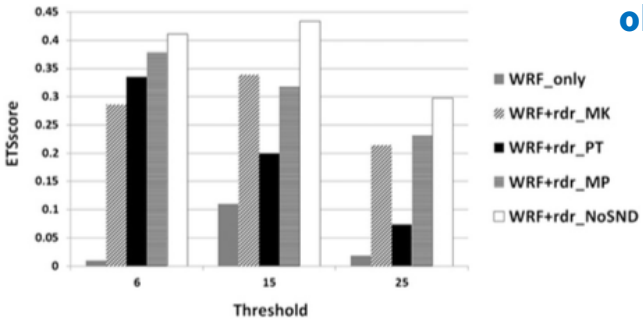

FIG. 15. ETS scores with thresholds of 6, 15, and 25 mm $(3\,\mathrm{h})^{-1}$ for all real case experiments.

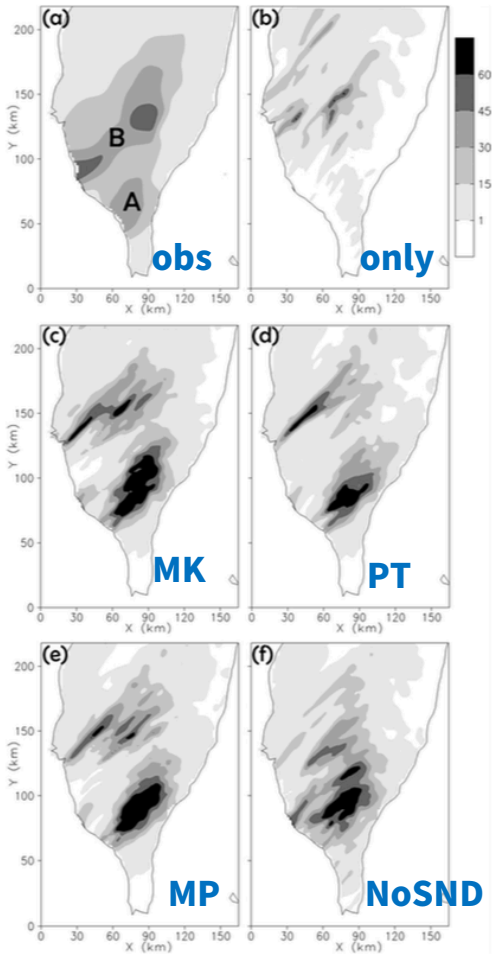

FIG. 14. The 3-h accumulated rainfall distributions over Taiwan from (a) observation, (b)WRF_only, (c)WRF+rdr_MK, (d)WRF+rdr_PT, (e)WRF+rdr_MP, and (f)WRF+rdr_NoSND.